Optics Communications ■ (■■■■) ■■■–■■■

Contents lists available at ScienceDirect

Optics Communications

journal homepage: www.elsevier.com/locate/optcom

Effect of frequency chirp on supercontinuum generation in silicon waveguides with two zero-dispersion wavelengths

Q1 Yanmei Cao, Libin Zhang, Yonghao Fei, Xun Lei, Shaowu Chen

Q2 *State Key Laboratory on Integrated Optoelectronics, Institute of Semiconductors, Chinese Academy of Sciences, Beijing 100083, China*

ARTICLE INFO

Article history:
Received 28 April 2014
Received in revised form
14 August 2014
Accepted 18 August 2014

Keywords:
Supercontinuum generation
Initial chirp
Silicon-on-insulator
Nonlinear photonics
Self-phase modulation
Four-wave mixing

ABSTRACT

The influence of initial chirp on supercontinuum generation in SOI rib waveguide with two zero-dispersion wavelengths was studied numerically, based on the generalized nonlinear Schrödinger equation (GNSE). The full-width at half-maximum (FWHM) and the peak power of the pre-chirped hyperbolic secant in the simulation are 50 fs and 50 W, respectively. The simulation results indicate that a positive initial chirp makes the energy transfer to the normal dispersion zone by affecting self-phase modulation (SPM) and four-wave mixing (FWM) processes, and therefore enhances the supercontinuum bandwidth as well as improves the spectral flatness. In particular, at the optimal initial chirp parameter of $C=3$, the bandwidth at -10 dB level increases to about 1620 nm (from 1140 to 2760 nm), exceeding an octave-spanning.

1. Introduction

Supercontinuum is a kind of ultrabroad band optical source, which has important realistic and potential applications in many fields, such as optical communication, spectroscopy and optical coherence tomography [1–3]. Compared with the traditional nonlinear optical media, such as crystals, semiconductor optical amplifier and high-nonlinearity optical fibers, silicon optical waveguides based on SOI platform show significant advantages in supercontinuum generation. Firstly, the refractive index contrast between Si and air or SiO_2 is larger, which can impose strong confinement. Secondly, silicon nanowire waveguides have a smaller transverse cross section, so that a relatively lower optical power can realize a high optical power density, and therefore the power threshold for supercontinuum generation is decreased. Moreover, the third-order susceptibility $\chi^{(3)}$ of silicon is about 3∼4 orders of magnitude larger than that of SiO_2 in near-infrared spectral region, thus, the effective nonlinearity is greatly enhanced in silicon nanowire waveguides. Lastly, the dispersion characteristics of silicon nanowire waveguides are very sensitive to geometric dimensions, so we can obtain an ideal dispersion distribution by effectively control the waveguide geometries [4,5] to the benefit of supercontinuum generation.

Supercontinuum generation in silicon waveguides has been widely investigated and a series of experimental as well as theoretical progresses have been reported. In 2004, Jalali et al. for the first time obtained a 2-fold spectral broadening in their experiment by using ∼4 ps optical pulse and demonstrated spectral broadening due to SPM effect [6]. In 2007, Yin et al. showed through numerical simulations that silicon waveguide can be used to create a supercontinuum with the bandwidth extending over 400 nm by launching femtosecond pulses as high-order solitons [7]. In 2011, Kuyken et al. demonstrated the generation of supercontinuum extending from 1535 to 2525 nm in a 2 cm long silicon wire by pumping with mid-infrared picosecond pulses in anomalous dispersion regime [8]. In 2012, Zhang et al. proposed a novel silicon slot waveguide exhibiting four-zero dispersion wavelengths and demonstrated an octave-spanning supercontinuum, ranging from 1217 to 2451 nm, assisted by dispersive wave generation [4].

It is well known that supercontinuum generation in silicon waveguides is not only influenced by the nonlinear effects, such as SPM, two-photon absorption (TPA), soliton fission and dispersive wave generation, but also the input pulse parameters, such as peak power and pulse width [7,9,10]. In this paper, we numerically calculated the influence of the initial pulse chirp on the supercontinuum generation in SOI rib waveguides with two zero dispersion wavelengths (ZDWs). The simulation results show that a relatively large positive initial chirp enhances the spectrum broadening and improves the spectral flatness of the generated supercontinuum.

2. Numerical model

To study the dynamic evolution of femtosecond pulse in the SOI rib waveguides, we numerically calculated the generalized nonlinear Schrödinger equation (GNSE), shown as follows [7],

$$\frac{\partial A(z,T)}{\partial z}=\sum_{k\geq 2}\frac{i^{k+1}}{k!}\beta_k\frac{\partial^k A}{\partial T^k}-\frac{1}{2}(\alpha_l+\alpha_f)A+i\gamma\left(1+i\tau_{shock}\frac{\partial}{\partial T}\right)$$

http://dx.doi.org/10.1016/j.optcom.2014.08.043
0030-4018/

$$\times A(z,T)\int_{-\infty}^{\infty} R(t)\left|A(z,T-t)\right|^2 dt \quad (1)$$

where $A=A(z, T)$ is the pulse envelope and T is a delayed time parameter measured in the reference frame moving with the envelop group velocity at the pump frequency. The first term on the right-hand side of Eq. (1) refers to the dispersion effect in silicon waveguides and β_k is the *kth* order dispersion coefficient by performing a Taylor-series expansion of the propagation constant around a center frequency ω_0; the second term denotes the linear loss and the free-carrier absorption (FCA) effect, with α_l and α_f accounting for the linear loss coefficient and the FCA coefficient, respectively; the third term represents nonlinear effects, where γ denotes the nonlinear coefficient. As for silicon, γ is defined as $\gamma=2\pi n_2/\lambda_0 A_{eff}+i\beta_{TPA}/2A_{eff}$, where n_2 and β_{TPA} are the Kerr coefficient and the TPA coefficient, respectively. A_{eff} is the mode effective area and $\tau_{shock}=1/\omega_0$ is the shock coefficient. $R(t)$ appearing in Eq. (1) is the nonlinear response function, which consists of the nearly instantaneous electronic response and the delayed Raman response. Similar to the case of silica fibers, we use the form $R(t)=(1-f_R)\delta(t)+f_R h_R(t)$, where f_R is the fractional contribution of the nuclei to the total nonlinear polarization and $h_R(t)$ is the Raman response function, which can be written as [11]

$$h_R(t)=\Omega_R^2\tau_1\exp(-t/\tau_2)\sin(t/\tau_1)\Theta(t) \quad (2)$$

where $\tau_2=1/\Gamma_R$ and $\tau_1=1/\sqrt{\Omega_R^2-\Gamma_R^2}\approx 1/\Omega_R$. The Raman-gain bandwidth Γ_R/π of 105 GHz in silicon corresponds to a response time of $\tau_2\approx 3$ ps. Similarly, the Raman frequency shift $\Omega_R/2\pi$ of 15.6 THz corresponds to $\tau_1\approx 10fs$. According to the normalization condition $\int_0^\infty h_R(t)dt=1$, the parameter f_R is found to be 0.043. $\Theta(t)$ is the Heaviside step function and $\delta(t)$ is the unit impulse function.

In our numerical model, the initial input pulse is assumed to have a hyperbolic secant field profile, which is shown as

$$A(0,t)=\sqrt{P_0}\,\mathrm{sec}\,h(t/T_0)\exp(-iCt^2/T_0{}^2) \quad (3)$$

where P_0 is the peak power, and C is the initial chirp parameter. The initial chirp can be imposed on by a proper phase modulation of the input pulse while maintaining constant pulse duration [12]. $T_0=T_p/2\ln(1+\sqrt{2})$ is the pulse width, where T_p is the temporal full-width at half-maximum (FWHM) of the input pulse. In our simulation, $P_0=50$ W and $T_p=50$ fs.

Several approaches [13] can be used to solve Eq. (1), such as the finite-difference time-domain (FDTD) method [17,18,19], the inverse scattering method [20], various perturbation techniques [21], Runge–Kutta schemes [22] and the split-step Fourier method (SSFM) [23,24]. In general, the SSFM is the most efficient because of its inherent stability and reasonable calculation speed.

3. Simulation results and discussion

We investigate the silicon waveguide with a rib transverse cross, as shown in Fig. 1. The silicon waveguide has an upper silica cladding layer and a lower silica boxing layer, with the width $W=0.5$ μm, the height $H=0.3$ μm, $r=h/H=0.2$ and the waveguide length $L=8$ mm.

In our simulation, a full-vector finite element algorithm is utilized to obtain the mode effective index $n_{eff}(\omega)$ for the fundamental quasi-TE mode, with material dispersion [13,14] of Si and SiO_2 taken into account. Then the modal propagation constant $\beta(\omega)$ can be obtained through the definition $\beta(\omega)=n_{eff}(\omega)\omega/c$, and the *kth* order dispersion coefficient is finally calculated via numerical differentiation from $\beta_k=d^k\beta/d\omega^k$. The wavelength dependence of n_{eff} and the second-order dispersion β_2 are shown in Fig. 2.

As shown in Fig. 2, the effective index of the TE mode decreases from 2.93 to 2.49 as the wavelength varies from 1.3 to 1.8 μm and the SOI rib waveguide exhibits two zero dispersion wavelengths (ZDWs)

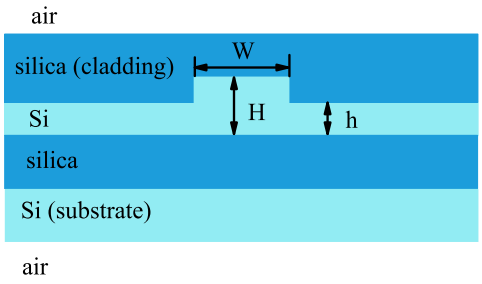

Fig. 1. Transverse cross section of silicon rib waveguide.

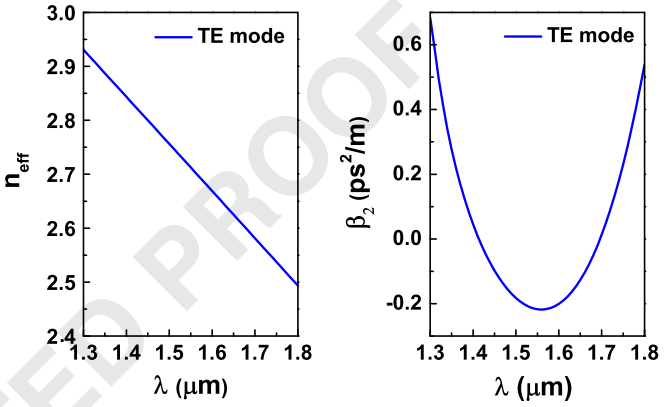

Fig. 2. Effective mode index (left) and GVD coefficient (right) of the fundamental TE mode.

which are located at 1.413 μm and 1.696 μm, respectively, thus the pulse center wavelength $\lambda_0=1.55$ μm is in the anomalous dispersion region. Up to tenth order dispersions are taken into account in our numerical simulation, and the dispersion coefficients at 1.55 μm are listed as follows: $\beta_2=-0.2172$ ps^2/m, $\beta_3=1.2191\times10^{-4}$ ps^3/m, $\beta_4=9.6242\times10^{-7}$ ps^4/m, $\beta_5=$-9.5701 $\times10^{-9}$ ps^5/m, $\beta_6=7.4948\times10^{-11}$ ps^6/m, $\beta_7=$-5.9124 $\times10^{-13}$ ps^7/m, $\beta_8=4.9423\times10^{-15}$ ps^8/m, $\beta_9=-4.4379\times10^{-17}$ ps^9/m and $\beta_{10}=4.2928\times10^{-19}$ ps^{10}/m. TPA coefficient is $\beta_{TPA}=5\times10^{-12}$ m/W, Kerr coefficient is $n_2=6\times10^{-18}$ m^2/W and the effective mode area is $A_{eff}=0.23$ μm^2. Thus, nonlinear coefficient is $\gamma=107+11i$ (m W)$^{-1}$. The order of the soliton excited by the input pulse satisfies the condition of $N=T_0\sqrt{\mathrm{Re}(\gamma)P_0/|\beta_2|}$, in our simulation, $N=8$.

The linear loss coefficient is set to be $\alpha_l=2$ dB/cm. FCA coefficient and free-carrier induced index change are $\alpha_f=\sigma_\alpha N_c$ and $n_f=\sigma_n N_c$, respectively, where $\sigma_n\approx$ -5.3 $\times10^{-21}$ cm^3, $\sigma_\alpha=1.45\times10^{-17}$ cm^2 and N_c is the free-carrier density. N_c can be obtained by solving Eq. (4):

$$\frac{\partial N_c(z,t)}{\partial t}=\frac{\beta_{TPA}}{2h\upsilon_0 A_{eff}^2}\left|A(z,t)\right|^4-\frac{N_c(z,t)}{\tau_c} \quad (4)$$

Here, τ_c is the effective lifetime of free carriers and it is estimated to be about 1 ns. By solving Eq. (4), we estimate a maximum free carriers density of $N_c\approx1.2\times10^{22}$ cm^{-3}, resulting in $\alpha_f\approx17.4$ m^{-1} and $n_f=-6.36\times10^{-5}$, both being too small to affect the propagation of femtosecond pulse.

With all described above, we study the dynamic evolution of input pulse in silicon waveguide by solving Eq. (1) with the split-step Fourier method (SSFM).

To study the influence of initial chirp on supercontinuum generation in silicon rib waveguides, we firstly calculate the bandwidth at −10 dB level and intensity distribution of output spectrum according to different initial chirp parameters, as shown in the Fig. 3.